Electro-oxidation of acetaminophen on nickel/poly(o-aminophenol)/multi-walled carbon nanotube nanocomposite modified graphite electrode

Ali Naeemy[1], Ali Mohammadi[1,2], Hedieh Bakhtiari[1], Nasim Ashouri[1], Roderick Bryan Walker[3]

[1]Department of Drug and Food Control, Faculty of Pharmacy, Tehran University of Medical Sciences,
Tehran, P.O. Box 14155-6451, Iran
[2]Nanotechnology Research Centre, Faculty of Pharmacy, Tehran University of Medical Sciences,
Tehran, P.O. Box 14155-6451, Iran
[3]Faculty of Pharmacy, Rhodes University, Grahamstown 6140, South Africa
E-mail: alimohammadi@tums.ac.ir

Poly(o-aminophenol) (POAP)/multi-walled carbon nanotube (MWCNT) nanocomposite and POAP in the absence of the MWCNT were fabricated by consecutive cyclic voltammetry (CV) on a graphite (G) electrode. The dispersion of nickel (II) ions was accomplished and incorporated into the polymeric electrodes (G/POAP and G/POAP-MWCNT) by immersing them into a 0.1 M nickel (II) solution. Following preparation of G/POAP/Ni and G/POAP-MWCNT/Ni, the electrochemical behaviour was examined using CV. Scanning electron microscopy was used for characterisation of the nanocomposite. The prepared electrodes showed enhanced electrocatalytic activity for the oxidation of acetaminophen and facilitated the detection of acetaminophen in a 0.1 M NaOH solution. Compared with the G/POAP/Ni electrode, the G/POAP-MWCNT/Ni electrode had a significant current response of acetaminophen oxidation because of the synergistic effects of POAP and the MWCNT. By CV, the calibration plot was linear in the range of 1–13 mM with standard deviation between 0.3 and 6.54% for acetaminophen. The G/POAP-MWCNT/Ni was successfully applied for acetaminophen determination in tablets and the results showed sufficient precision and achieved a mean recovery of 96.8% (R.S.D. = 4.9%).

1. Introduction: Since electrochemical methods of analysis are simple, rapid and economical, they are widely used to determine electroactive compounds in biological fluids and pharmaceutical dosage forms [1]. Acetaminophen, N-acetyl-p-aminophenol (APAP), is an analgesic anti-pyretic compound so that it could be appropriate for treating patients allergic to aspirin. The compound can be used for relieving backache, headache and post-operative arthritic pain [2]. However, APAP has been used in suicide attempts as large doses can damage the kidneys and liver and may eventually lead to death [3, 4].

Consequently, it may be useful to develop a rapid, credible, specific and sensitive method for the analysis of APAP in biological fluids. A variety of existing techniques such as spectrofluorimetry [5], spectrophotometry [6, 7], chromatography [8, 9] and electrochemical approaches are applied to the analysis of APAP [10–13]. In recent years, numerous electrochemical methods have been applied to the detection of APAP in pharmaceutical dosage forms or biological fluids [14–22]. Different materials including poly(Patton and Reeder's reagent) [14], plant tissue [15] and nanomaterials made of carbon nanotubes (CNTs) [3, 4, 16–22] have been applied. The mode of nanomaterial application to the surface of the electrodes permits differentiation of the electrode in respect of the proficiency of rapid electron transfer mediation [23–25]. Furthermore, electrode modification with conductive polymers compared to nanoparticulate makes it simple and easy to fabricate modified electrodes [26–29].

Previously a modified graphite (G) electrode with poly (o-aminophenol) (POAP)/nickel (Ni) was used for the oxidation of saccharose in an alkaline electrolyte medium [26]. The useful characteristics of modified polymeric films through the incorporation of metallic particles have been combined to fabricate a conductive polymer in a modified electrode system. Multi-walled CNTs (MWCNTs) have a reticular structure that exhibit a high level of stability with an accessible and large surface area, a narrow size distribution and low impedance [30, 31]. Recent studies have shown that the application of CNTs to a polymer matrix can improve electric conductivity while retaining the mechanical characteristics of the original polymer matrix [32]. The redox properties of conductive polymers have been enhanced through the use of CNTs because of their large surface area and therefore a new polymer composite with MWCNTs was developed [32].

In the work reported in this Letter, POAP was synthesised by consecutive cyclic voltammetry (CV) in an o-aminophenol (OAP) solution in the presence and absence of a MWCNT on the surface of the G electrode. Subsequently, Ni (II) ions were incorporated into the G/POAP, G/POAP-MWCNT electrodes by immersion into a 0.1 M Ni (II) ion solution. Electrochemical studies of G/POAP/Ni and G/POAP-MWCNT/Ni electrodes were undertaken using a cyclic voltammetric technique. The electrodes that had been developed were used for electrocatalytic oxidation of APAP in a 0.1 M NaOH solution and the practical application of the G/POAP-MWCNT/Ni electrode was demonstrated by analysis of APAP in tablets.

2. Experimental

2.1. Reagent and materials: Sodium hydroxide, OAP, perchloric acid, nickel sulphate were purchased from Merck (Darmstadt, Germany). All reagents were at least of analytical grade and were used without further purification. MWCNTs (diameter < 10 nm, length 5–15 μm, surface area 180–190 m^2g^{-1} and amorphous carbon <3%) were purchased from the Neutrino Co. (Tehran, Iran). All aqueous solutions were prepared using double distilled water.

APAP was donated by the Iranian Quality Control Laboratory of the Ministry of Health and the Medical Education Department, Tehran, Iran. Commercially available APAP tablets (each tablet containing 500 mg acetaminophen) were purchased from local pharmacies.

2.2. Instrumentation: Electrochemical studies were performed using a conventional three-electrode cell powered by a μ-AUTOLAB TYP III. A dual-Ag/AgCl saturated KCl electrode (Metrohm) [+197 mV against SHE] and a platinum (Pt) rod were used as the reference and counter electrodes, respectively. The

working electrode was a G-disk electrode (Azar Electrode Co., Iran) with an exposed surface area of 0.0314 cm^2. The surface morphology of the modified electrode was determined by field emission scanning electron microscopy (FE-SEM, S-4160, Hitachi, Japan). All data were generated at an ambient temperature of 25°C.

2.3. Electropolymerisation procedure: Prior to manufacture, the G electrode was polished with 0.05 mm alumina powder on a polishing microcloth and subsequently rinsed thoroughly with distilled water. The control films of POAP and the POAP-MWCNT on the G electrode were fabricated using two electro-polymerisation baths maintained under similar electrochemical conditions at 25°C in a glass cell, under CV conditions of 50 cycles at a scan rate of 100 mVs^{-1} between −0.3 and 1.2 V.

The G/POAP electrode was manufactured by modification of the G electrode surface with a conducting electro-polymerisation solution containing the OAP monomer (5 mM in 0.1 M HClO$_4$). The G/POAP-MWCNT electrode was also prepared as the G/POAP electrode in the presence of different ratios of MWCNTs ranging between 1 and 15% w/w).

2.4. Incorporation of Ni (II) ions into the polymeric matrix: The manufactured G/POAP and G/POAP-MWCNT electrodes were carefully placed into an open circuit in a 0.1 M nickel sulphate aqueous solution that was stirred. A complex was formed between the amine functional sites of the polymeric film backbone and Ni (II) using an accumulation time (τ_a) of 40 min [26, 33].

3. Results and discussion

3.1. Effect of MWCNTs on electrochemical polymerisation: The preparation of POAP films on the surfaces of substrates such as platinum (Pt) and glassy carbon (GC) electrodes using cyclic voltammetric methods has been reported [34–38]. The oxidation products of OAP (3-aminophenoxazone (3APZ) [38] and 2,2-dihydroxyazobenzene) were detected using SERS spectra (Figs. 1a and b, 3APZ and phenoxazine units) [36, 37].

The consecutive cyclic voltammograms (CVs) (50 cycles) for the electropolymerisation of OAP in the absence of MWCNTs are shown in Fig. 2a. An anodic peak can be observed at approximately 950 mV for OAP and no corresponding cathodic peaks were observed in the reverse scan, implying that the monomer had undergone irreversible oxidation. At lower oxidation potentials, two pairs of redox peaks that are related to 3APZ and POAP were observed during subsequent cycles of exposure.

The current observed during monomer oxidation intensified following the addition of MWCNTs to the solution (Fig. 2b). In addition, the peak for POAP increased simultaneously as the peak for 3APZ intensified and the rate of polymerisation increased considerably because of the enhancement of the current associated with the redox peaks. Furthermore, when potential cycling was continued for an additional two or more cycles, the peak size and the current increased. Increasing the number of scans resulted in an increase in the current, indicating the progressive enrichment of electroactive monomer species on or near the surface of the electrode. Accordingly, in the presence of MWCNTs, the monomer produces increasing amounts of monocation radicals that can reach the surface of the electrode relatively easily.
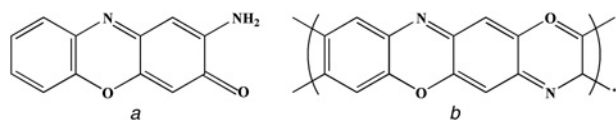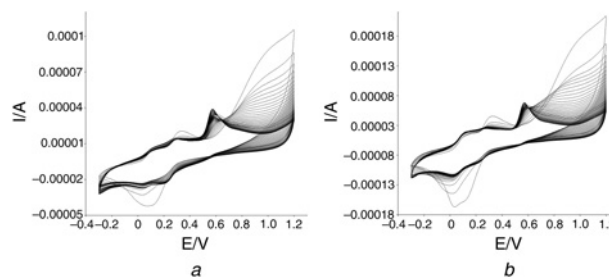

Figure 2 *Electropolymerisation of POAP in 5 mM OAP monomer/0.1 M HClO$_4$ solution on surface of graphite electrode in absence (Fig. 2a) and in presence (Fig. 2b) of 8% w/w MWCNTs obtained at scan rate of 100 mV s^{-1}*

3.2. FE-SEM observations: Fig. 3a shows the typical FE-SEM image of the G/POAP/Ni. After the formation of OAP film, a compact and uniform layer was acquired. The G/POAP-MWCNT/Ni suggest that the majority of MWCNTs have been entrapped in the POAP film (Fig. 3b), thus the three-dimensional (3D) film structure and homogenous nanocomposite film obtained indicate a strong interaction between the Ni, MWCNTs and polymer [35]. The Ni come into sight as grown spots embedded in the POAP-MWCNTs. In addition, it is clear from the image that the nanocomposite morphologies have approximately equal sizes in the micrometre to several hundred nanometre scales. A very high magnification of the FE-SEM image shows the presence of light cylindrical spots in G/POAP-MWCNT/Ni, which are distributed all over the nanocomposite.

3.3. Electrochemical behaviour of G/POAP/MWCNT and G/POAP electrodes: Following the formation of the polymeric film, the electrodes were removed and rinsed with water to remove any remaining monomer on the surface. The electrochemical behaviour of the G/POAP/MWCNT and G/POAP electrodes was assessed by undertaking CV measurements in 0.1 M HClO$_4$ (see Fig. 4).

The CV of the G/POAP/MWCNT electrode [Fig. 4 (3)] revealed the presence of a pair of broad and intense redox peaks. The peak current was more intense in comparison to that observed for with the G and G/POAP electrodes [Fig. 4 (1) and (2)], which is more likely because of the presence of MWCNTs. Comparison of the difference in the ratio of MWCNTs to POAP growth shows that the current associated with the anodic peak in the tenth cycle at 0.35 V in relation to 3APZ was used as an index of the rate of polymerisation.
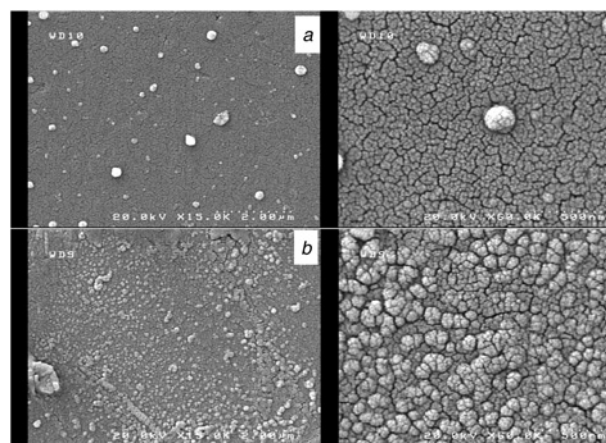
Figure 3 *FE-SEM images of G/POAP/Ni (Fig. 3a) and G/POAP-MWCNT/ Ni (Fig. 3b)*
Right side of Figure is the magnified FE-SEM image

Figure 1 *Structure of 3APZ (Fig. 1a) and phenoxazine (Fig. 1b) units*
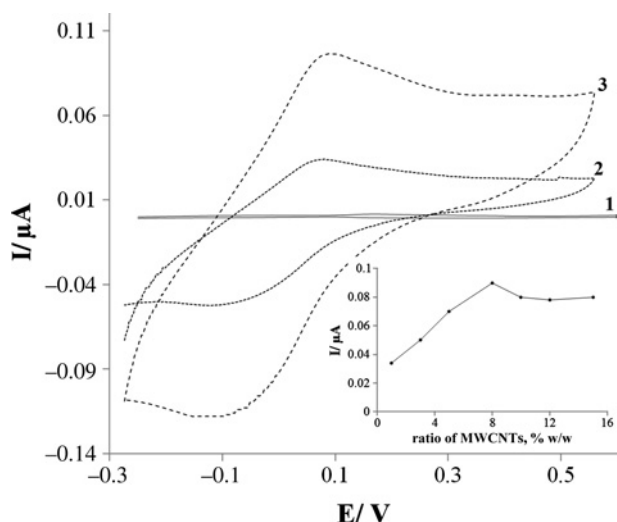
Figure 4 *CVs of G (1), G/POAP (2) and G/POAP-MWCNT (3) in 0.1 M HClO₄ generated at scan rate of 100 mV s⁻¹*
Inset: Amount of anodic peak current of this electrochemical response against MWCNT ratio for electropolymerisation of 5 mM OAP

Different percentages of MWCNTs (1% up to 15% w/w) were added to an OAP solution and it was shown that incremental increases in the concentration of MWCNTs led to a rapid increase in the rate of polymerisation and that saturation was observed at approximately 8% w/w loading as depicted in the inset of Fig. 4. It is clear that at concentrations of MWCNTs <8% w/w, no remarkable difference in the rate of polymerisation is observed in comparison to when no MWCNTs are present. An excess of MWCNTs in ratios between 8 and 15% w/w monomer solutions also did not appear to have an effect on the rate of polymerisation (Fig. 4, inset) and therefore a concentration of 8% w/w MWCNTs in the monomeric solution was used to manufacture the modified electrode.

3.4. Electrochemical activation of G/POAP-MWCNT/Ni and G/POAP/Ni electrodes: Successive CVs of G/POAP/Ni and G/POAP-MWCNT/Ni electrodes in a 0.1 M NaOH solution generated at a scan rate of 100 mVs⁻¹ are depicted in Figs. 5a and b, respectively. These CVs permitted evaluation of the formation of nickel hydroxide film in parallel to the electrochemical reactivity of the surface of the electrodes. The initial scan revealed a pair of oxidation and reduction peaks, at 495 and 407 mV/Ag, AgCl, which were attributed to the Ni²⁺/Ni³⁺ redox couple in alkaline media, which has been reported in previous studies with related species [13, 26, 29].

During sequential cycling, the peaks shifted to negative potential and were fixed at 473 and 388 mV/Ag, AgCl, respectively. These observations are similar to previously reported studies in which
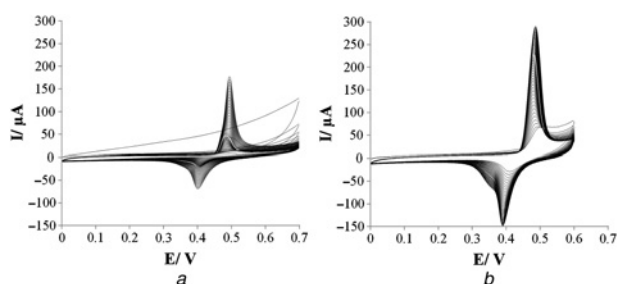
the interconversion and the formation of the α and β-phases of Ni(OH)₂, conversion to NiOOH and the enrichment of Ni³⁺ species on or just beneath the surface were discussed [39–43]. The oxygen evolution reaction (OER) was clearly inhibited as additional continuous cycle exposure was achieved, while the intensity remained unchanged [44, 45].
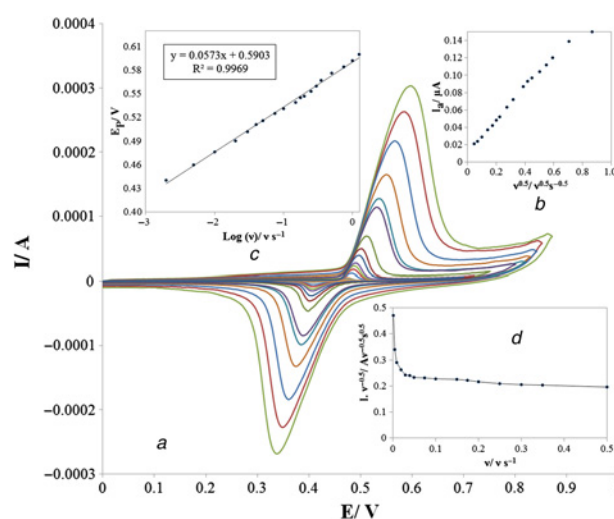
A typical CV of the G/POAP-MWCNT/Ni electrode in 0.1 M NaOH solution at different potential sweep rates of 2–1500 mV s⁻¹ is depicted in Fig. 6a, and the current response against the square root of the corresponding potential sweep rate in linear mode is depicted in Fig. 6b and indicates the conquest of diffusion controlled processes. In addition, the electrochemical activity of the surface redox peak should be evaluated. From the slope of the line using the following equation [1, 46]

$$I_p = \left(\frac{n^2 F^2}{4RT}\right) nA\Gamma^* \tag{1}$$

where v is the potential sweep rate taking the average of both the cathodic and the anodic results and Γ^* is the surface concentration of the redox species in the film per unit surface area of the electrode, Γ^* values can be derived and were $\sim 4.6 \times 10^{-8}$ and 1.2×10^{-8} mol cm⁻² for the G/POAP-MWCNT/Ni and G/POAP/Ni electrodes, respectively. These values correspond to the presence of 75 and 40 monolayers of surface species for Ni in the presence and absence of MWCNTs, respectively.

Graphical representations of peak potentials pertaining to the logarithm of the potential sweep rate are located in Fig. 6c. The values of E_p depend linearly on the logarithm of the potential sweep rate as shown by Laviron, who derived general expressions for the linear potential sweep of the voltammetric response of a surface confined electro-reactive species [47]. The expressions for peak-to-peak potential separation (E_p) can be mathematically determined using the following equations

$$E_p = E^0 + \left[\frac{RT}{(1+\alpha_s)nF}\right]\ln\left(\frac{1-\alpha_s}{Y}\right) \tag{2}$$

Figure 5 *Consecutive CVs of 100 mM NaOH solution using G/POAP/Ni (Fig. 5a) and G/POAP-MWCNT/Ni (Fig. 5b) electrodes*
Potential sweep rate was 100 mV s⁻¹ and cycle number increases from inner to outer peaks

Figure 6 *Typical CVs of G/POAP-MWCNT/Ni electrode in 0.1 M NaOH using potential sweep rates of 2–1500 mV s⁻¹ (Fig. 6a); proportionality of anodic peak currents to square roots of sweep rate (Fig. 6b); plot of E_p against log v for CVs depicted for anodic peak current in Fig. 5a (Fig. 6c); dependency of normalised peak current on sweep rate (Fig. 6d)*

where

$$Y = \left(\frac{RT}{F}\right)\left(\frac{k_s}{n\nu}\right) \qquad (3)$$

where E_p is the anodic peak potential, ν is the potential sweep rate and k_s is the obvious charge-transfer rate constant. Using (2) and (3) and by plotting E_p against ν, the α_s (anodic electron-transfer coefficient) can be measured.

The value for k_s can be determined by measuring E_p values for the electron transfer across the G/POAP-MWCNT/Ni/solution interface. Using the graphical representation and (2) and (3), the average value of k_s was found to be 1.62 s^{-1} with a corresponding value of α_s of 0.8. The normalised current response determined as the current response multiplied by the square root of the corresponding potential sweep rate is depicted in Fig. 6d, indicating that diffusion controlled processes are dominant.

3.5. Electrocatalytic oxidation of APAP by G/POAP-MWCNT/Ni and G/MWCNT/Ni electrodes: Typical CVs generated using modified electrodes in 0.1 M NaOH solution in the absence and presence of 4 mM APAP at a potential sweep rate of 10 mV s^{-1} in the potential range between 0 and 700 mV/Ag, AgCl are depicted in Fig. 7. As shown, a well-developed redox peak was observed on the G/POAP/Ni and G/POAP-MWCNT/Ni electrodes, whereas on the uncoated G, G/POAP and G/POAP-MWCNT electrodes (Fig. 7) no oxidation nor reduction was observed for APAP.

In contrast, a well-developed redox wave for APAP on the G/POAP/Ni electrode was observed as the emergence of a new peak at a lower negative potential of about 220 mV/Ag, AgCl. A comparison of the responses observed for the G/POAP/Ni electrode and the G/POAP-MWCNT/Ni electrode revealed that the anodic peak for APAP increases, indicating that the G/POAP-MWCNT/Ni electrode has a better electrocatalytic effect for the oxidation of APAP and improves the catalytic characteristics of nickel oxide through the penetration of the fine catalyst particles into the nanocomposite polymeric matrix with an associated increase in the surface area. Since the anodic peak current of the low-valence nickel species is enhanced, the cathodic current decreases simultaneously.

These results suggest that APAP was oxidised by an EC' mechanism via an oxyhydroxide species that is immobilised on the surface of the electrode. The mechanism is based on the continuous consumption of the reactive species by APAP and electrochemical generation of Ni (III) active sites in the solution.

Nonetheless, the number of consecutive CVs for the 50 cycles and the time of nickel dispersion (40 min) for G/POAP/Ni and G/POAP-MWCNT/Ni electrodes were similar, which may be because of the peak current for the oxidation of APAP on the surface of the G/POAP-MWCNT/Ni electrode being greater than that for the G/POAP/Ni electrode because of greater conductivity, a larger real surface area and faster polymer deposition on the G/POAP-MWCNT/Ni electrode.

The CV response of the G/POAP-MWCNT/Ni in the presence of different concentrations of APAP is shown in Fig. 8. Following the addition of APAP, an increase in the anodic current for the G/POAP-MWCNT/Ni electrode occurs. The electrocatalytic response for APAP was considered suitable for the purposes of quantification of the APAP. The anode current was observed to increase, followed by a decrease in the cathodic charge, with increasing amounts of APAP. The anodic peak current on the concentration plot suggests linear behaviour in the typical calibration range of 1–13 mM with a resultant correlation coefficient of 0.998.

The percentage RSD values ranged between 0.3 and 6.54% for three calibration curves and a curve of $I_{pa} = 0.9254\,C + 1.1738$ ($R^2 = 0.998$) is a typical regression equation that could be utilised for the continuation of APAP.

The anodic current is dependent upon the concentration of APAP (Fig. 8, inset) and a change in the concentration of APAP led to a linear change in the anodic current; thus it can be concluded that the catalysis of APAP on the G/POAP-MWCNT/Ni electrode is specific.

The precision of the method was evaluated with respect to reproducibility (multiple electrodes) and repeatability (single electrode). The repeatability was examined by continuous electrocatalytic APAP oxidation using the same G/POAP-MWCNT/Ni electrode for the analysis of a standard solution ($n = 6$). The anodic peak current reduced by 0.6% after six complete scans, which suggests that the electrode can be successfully used for repeat analysis without a detrimental impact on the surface characteristics of the electrode. The reproducibility of the system was established by analysis of three replicate ($n = 3$) standard samples containing 3, 7 and 12 mM of APAP on three consecutive days. The averages of the measured concentrations were found to be 3.2, 7.1 and 11.3 mM with % R.S.D. values of 4.12, 1.06 and 7.25, respectively.
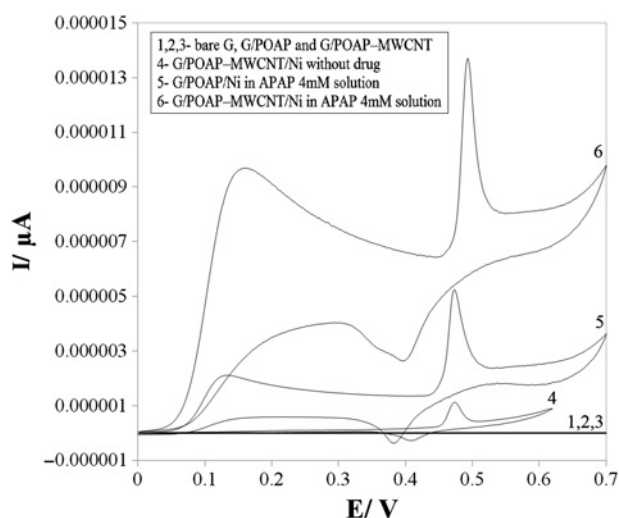
Figure 7 *CVs in absence and presence of 4 mM of APAP on various electrodes in 0.1 M NaOH solution at potential sweep rate of 10 mV s^{-1}*
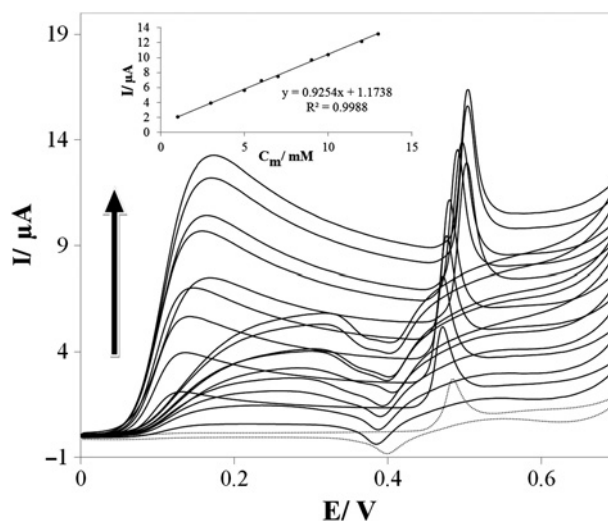
Figure 8 *CVs of G/POAP-MWCNT/Ni electrode in 0.1 M NaOH solution in presence of 1–10 mM APAP in solution*
Potential sweep rate was 10 mV s^{-1}
Inset: Dependency of anodic peak current on concentration of APAP in solution

The assessment of accuracy was achieved by analysis of the same three replicate standard samples that were used to establish reproducibility and the percentage relevant errors ranged between –5.83 and 6.66% and were deemed acceptable.

The CVs for a 4 mM APAP solution generated using a G/POAP-MWCNT/Ni electrode at different potential sweep rates are depicted in Fig. 9. The inset of Fig. 9 reveals that the anode current is dependent on the square root of the corresponding potential sweep rate and increased in a linear fashion.

This phenomenon suggests that the mass transfer process of oxidation is controlled by diffusion; by use of (4) the electron transfer coefficient for the reaction can be established and is valid for an irreversible diffusion controlled process [1]

$$E_p = \left(\frac{RT}{n\alpha F}\right)\ln \nu = \text{constant} \tag{4}$$

The use of the dependence of peak potential on the natural logarithm of potential sweep rate permits the determination of electron transfer coefficients for APAP, which were 0.58 and 0.41 for the G/MWCNT/Ni and G/POAP-MWCNT/Ni electrodes, respectively

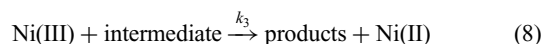$$I_p = 2.99 \times 10^5 n^{3/2} \alpha^{1/2} C D^{1/2} \nu^{1/2} \tag{5}$$

where I_p is the peak current, C is the bulk concentration of APAP and D is the diffusion coefficient. The slope of the linear plot of the anodic peak current and the square root of potential sweep rates (Fig. 9, inset) and the use of the Randles-Sevcik (5) [1] facilitated the identification of the diffusion coefficients for APAP that were 3×10^{-6} and 5.90×10^{-6} cm^2 s^{-1} for the G/MWCNT/Ni and G/POAP-MWCNT/Ni electrodes, respectively.

Based on these results, the following mechanism proposed for mediated oxidation of APAP on the G/POAP-MWCNT/Ni electrode's surface for which the corresponding kinetics for the redox transition of the nickel species can be proposed

$$\text{Ni(II)} \xrightarrow{k_2, k_{-2}} \text{Ni(III)} + e^- \tag{6}$$
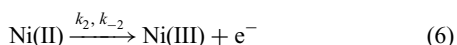
is followed by the oxidation of drugs on the modified surface via the

reaction

$$\text{Ni(III)} + \text{Drug} \xrightarrow{k_1} \text{Intermediate} + \text{Ni(II)} \tag{7}$$

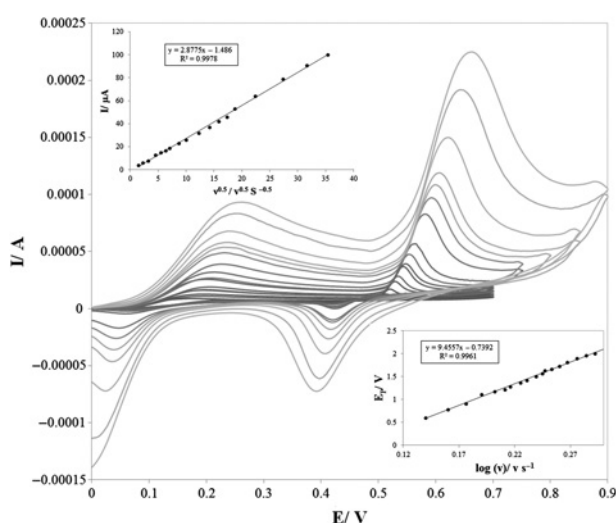$$\text{Ni(III)} + \text{intermediate} \xrightarrow{k_3} \text{products} + \text{Ni(II)} \tag{8}$$

3.6. Analytical application of modified electrode: To confirm the application of the proposed method, the analysis of commercial APAP tablets was undertaken. 20 tablets were weighed, finely powdered and mixed. An amount of powder equal to the weight of one tablet was transferred to an A-grade volumetric flask, dissolved in double distilled water with sonication for 30 min. The solution was made up to volume with double distilled water. The result of the assay of the APAP tablets yielded a recovery of 96.8% (R.S.D. = 4.9%) of that claimed on the label with a percentage relevant error of –3.2%; the values measured using this method were in agreement with previously reported values [4, 25].

4. Conclusion: Owing to the unique properties of MWCNTs such as high specific surface area, G/POAP/Ni and G/POAP-MWCNT/Ni modified electrodes were prepared for the determination of APAP. The electrodes were fabricated by electropolymerisation of OAP on a G electrode in the absence and presence of MWCNTs. The electrodes revealed that electrocatalytic oxidation of APAP was predominant and the large current response of APAP on the G/POAP-MWCNT/Ni electrode when compared to that observed for the G/POAP/Ni electrode could be attributed to the synergistic effect of POAP and the MWCNTs in the system. Through the use of CV, the kinetic parameters of APAP such as charge-transfer coefficient, catalytic reaction rate constant and diffusion coefficient for oxidation were established. The proposed nanocomposite polymeric film is a simple, new and effective electrode that has been applied to measure APAP in pharmaceutical preparations.

Figure 9 *Typical CVs of G/POAP-MWCNT/Ni in 0.1 M NaOH in presence of 4 mM APAP at potential sweep rates between 2 and 1250 mV s⁻¹*
Upper inset: Dependence of anodic peak current during forward sweep on square root of sweep rate
Lower inset: Dependence of peak potential on lnν for oxidation of APAP at G/POAP-MWCNT/Ni electrode

6 References

[1] Bard A.J., Faulkner L.R.: 'Electrochemical methods, fundamentals and applications' (Wiley, New York, 2001)
[2] Martindale W.A.: 'The extra pharmacopoeia' (The Pharmaceutical Press, London, 1979, 27th edn)
[3] Ghorbani-Bidkorbeh F., Shahrokhian S., Mohammadi A., ET AL.: 'Simultaneous voltammetric determination of tramadol and acetaminophen using carbon nanoparticles modified glassy carbon electrode', *Electrochim. Acta*, 2010, **55**, (8), pp. 2752–2759
[4] Moghaddam A.B., Mohammadi A., Mohammadi S., ET AL.: 'The determination of acetaminophen using a carbon nanotube: graphite-based electrode', *Microchim. Acta*, 2010, **171**, pp. 377–384
[5] RuizMedina A., Fernandezde Cordoba L., Molina Diaz A.: 'A simple solid phase spectrofluorimetric method combined with flow analysis for the rapid determination of salicylamide and salicylic acid in pharmaceutical samples', *Fresenius J. Anal. Chem.*, 1999, **365**, pp. 619–623
[6] Vilchez J.L., Blanc R., Avidad R., ET AL.: 'Spectrofluorimetric determination of paracetamol in pharmaceuticals and biological fluids', *J. Pharm. Biomed. Anal.*, 1995, **13**, pp. 1119–1125
[7] Erk N., Ozkan Y., Banoglu E., ET AL.: 'Simultaneous determination of paracetamol and methocarbamol in tablets by ratio spectra derivative spectrophotometry and LC', *J. Pharm. Biomed. Anal.*, 2001, **24**, pp. 469–475
[8] Altun M.: 'HPLC method for the analysis of paracetamol, cafeine and dipyrone', *Turk. J. Chem.*, 2002, **26**, pp. 521–528
[9] Gros M., Petrović M., Barceló D.: 'Development of a multi-residue analytical methodology based on liquid chromatography-tandem mass spectrometry (LC-MS/MS) for screening and trace level

determination of pharmaceuticals in surface and wastewaters', *Talanta*, 2006, **70**, (4), pp. 678–690

[10] Speed D.J., Dickson S.J., Cairns E.R., ET AL.: 'Analysis of paracetamol using solid-phase extraction, deuterated internal standards, and gas chromatography-mass spectrometry', *J. Anal. Toxicol.*, 2001, **25**, pp. 198–202

[11] Junior Netogo L.R., Fernandez J.R., Kubata L.T.: 'Determination of salicylate in blood serum using an amperometric biosensor based on salicylate hydroxylase immobilized in a polypyrrole–glutaraldehyde matrix', *Talanta*, 2000, **51**, pp. 547–557

[12] Logman M.J., Budygin E.A., Gainetdinov R.R., ET AL.: 'Quantitation of in vivo measurements with carbon fiber microelectrodes', *J. Neurosci. Method*, 2000, **95**, (2), pp. 95–97

[13] Feizbakhsh A., Aghassi A., Naeemy A., ET AL.: 'Electrocatalytic oxidation of paracetamol on Ni and NiCu alloy modified glassy carbon electrode', *J. Chin. Chem. Soc.*, 2012, **59**, pp. 1086–1093

[14] Thomas T., Mascarenhas R.J., Cotta F., ET AL.: 'Poly(Patton and Reeder's reagent) modified carbon paste electrode for the sensitive detection of acetaminophen in biological fluid and pharmaceutical formulations', *Colloids Surf. B*, 2013, **101**, pp. 91–96

[15] Rounaghi G., Kakhki R.M.: 'Preparation and electrochemical application of a new biosensor based on plant tissue/polypyrrole for determination of acetaminophen', *Bull. Mater. Sci.*, 2012, **35**, (5), pp. 811–816

[16] Sun D., Zhang H.: 'Electrochemical determination of acetaminophen using a glassy carbon electrode coated with a single-wall carbon nanotube-dicetyl phosphate film', *Microchim. Acta*, 2007, **158**, pp. 131–136

[17] Li M., Jing L.: 'Electrochemical behavior of acetaminophen and its detection on the PANI–MWCNTs composite modified electrode', *Electrochim. Acta*, 2007, **52**, pp. 3250–3257

[18] Wan Q., Wang X., Yu F., ET AL.: 'Poly(taurine)/MWNT-modified glassy carbon electrodes for the detection of acetaminophen', *J. Appl. Electrochem.*, 2009, **39**, (6), pp. 785–790

[19] Li Y., Shi X., Hao J.: 'Electrochemical behavior of glassy carbon electrodes modified by multi-walled carbon nanotube/surfactant films in a buffer solution and an ionic liquid', *Carbon*, 2006, **44**, (13), pp. 2664–2670

[20] Silva M.L.S., Garcia M.B.Q., Lima J.L.F.C., ET AL.: 'Modified tubular electrode in a multi-commutated flow system: determination of acetaminophen in blood serum and pharmaceutical formulations', *Anal. Chim. Acta.*, 2006, **573**, pp. 383–390

[21] Umasankar Y., Unnikrishnan B., Chen S.M., ET AL.: 'Effective determination of acetaminophen present in pharmaceutical drug using functionalized multi-walled carbon nanotube film', *Int. J. Electrochem. Sci.*, 2012, **7**, (1), pp. 484–498

[22] Revanasiddappa M., Dodahalli H.N., Gurukar S.S., ET AL.: 'Electrochemical detection of acetaminophen on the functionalized MWCNTs modified electrode using layer-by-layer technique', *Electrochim. Acta*, 2011, **56**, pp. 6619–6627

[23] Mohammadi A., Moghaddam A.B.: 'Direct electrochemistry and electrocatalysis of immobilised cytochrome *c* on electrodeposited nanoparticles for the reduction of oxygen', *Micro Nano Lett.*, 2012, **7**, (9), pp. 951–954

[24] Mohammadi A., Moghaddam A.B., Kazemzad M., ET AL.: 'Synthesis of nickel oxides nanoparticles on glassy carbon as an electron transfer facilitator for horseradish peroxidase: direct electron transfer and H_2O_2 determination', *J. Mat. Sci. Eng. C*, 2009, **29**, pp. 1752–1758

[25] Mohammadi A., Moghaddam A.B., Dinarvand R., ET AL.: 'Bioelectrocatalysis of methyldopa by adsorbed tyrosinase on the surface of modified glassy carbon with carbon nanotubes', *Int. J. Electrochem. Sci.*, 2008, **3**, pp. 1248–1257

[26] Ehsani A., Mahjani M.G., Naeemy A.: 'Influence of ionic surfactant on physio-electrochemical properties and fractal dimension of poly ortho aminophenol film', *Prog. Org. Coat.*, 2010, **69**, (4), pp. 510–516

[27] Zheng Y., Du Q., He M., ET AL.: 'Synthesis and electrochemical properties of graphite oxide/MnO_2/conducting polymer ternary composite for supercapacitors', *Micro Nano Lett.*, 2012, **7**, (8), pp. 778–781

[28] Mahale B.P., Bodas D., Gangal S.A.: 'Development of low-cost poly (vinyldifluoride) sensor for low-pressure application', *Micro Nano Lett.*, 2011, **6**, (7), pp. 540–542

[29] Ehsani A., Mahjani M.G., Naeemy A.: 'Electrosynthesis of polypyrrole composite film and electrocatalytic oxidation of ethanol', *Electrochim. Acta*, 2012, **71**, pp. 128–133

[30] Mohammadi A., Moghaddam A.B., Alikhani E., ET AL.: 'Electrochemical quantification of fluoxetine in pharmaceutical formulation using carbon nanoparticles', *Micro Nano Lett.*, 2013, **8**, (12), pp. 853–857

[31] Mohammadi A., Moghaddam A.B., Eilkhanizadeh K., ET AL.: 'Electro-oxidation and simultaneous determination of amlodipine and atorvastatin in commercial tablets using carbon nanotube modified electrode', *Micro Nano Lett.*, 2013, **8**, (8), pp. 413–417

[32] Ehsani A., Mahjani M.G., Jafarian M.: 'An electrochemical study of the synthesis and properties of multi-walled carbon nanotube/poly ortho aminophenol composites', *Synthetic Met.*, 2011, **161**, pp. 1760–1765

[33] Delime F., Leger J.M., Lamy C.: 'Enhancement of the electrooxidation of ethanol on a Pt–PEM electrode modified by tin. Part I: Half cell study', *J. Appl. Electrochem.*, 1999, **29**, pp. 1249–1254

[34] Hernandez N., Ortega J.M., Choy M., ET AL.: 'Electrodeposition of silver on a poly(o-aminophenol) modified platinum electrode', *J. Electroanal. Chem.*, 2001, **515**, pp. 123–128

[35] Ortega J.M.: 'Conducting potential range for poly (o-aminophenol)', *Thin Solid Films*, 2000, **371**, pp. 28–35

[36] Jackowska K., Bukowska J., Kudelski A.: 'Electro-oxidation of o-aminophenol studied by cyclic voltammetry and surface enhanced Raman scattering (SERS)', *J. Electroanal. Chem.*, 1993, **350**, pp. 177–187

[37] Jackowska K., Bukowska J., Kudelski A.: 'Poly-ortho-aminophenol modified electrodes—structure and electrochemical properties', *Polish J. Chem.*, 1994, **68**, pp. 141–151

[38] Li Y., Chen S.M.: 'The electrochemical properties of acetaminophen on bare glassy carbon electrode', *Int. J. Electrochem. Sci.*, 2012, **7**, pp. 2175–2187

[39] El-Shafei A.A.: 'Electrocatalytic oxidation of methanol at a nickel hydroxide/glassy carbon modified electrode in alkaline medium', *J. Electroanal. Chem.*, 1999, **471**, (2), pp. 89–95

[40] Briggs G.W.D., Snodin P.R.: 'Ageing and the diffusion process at the nickel hydroxide electrode', *Electrochim. Acta*, 1982, **27**, (5), pp. 565–572

[41] Hahn F., Beden B., Croissant M.G., ET AL.: '*In situ* UV visible reflectance spectroscopic investigation of the nickel electrode-alkaline solution interface', *Electrochim. Acta*, 1986, **31**, (3), pp. 335–342

[42] Desilvestro J., Corrigan D.A., Weaver M.J.: 'Characterization of redox states of nickel hydroxide film electrodes by in situ surface Raman spectroscopy', *J. Electrochem. Soc.*, 1988, **135**, (4), pp. 885–892

[43] Barnard R., Randell C.F.: 'Studies concerning charged nickel hydroxide electrodes. VII. Influence of alkali concentration on anodic peak positions', *J. Appl. Electrochem.*, 1983, **13**, (1), pp. 89–95

[44] Conway B.E., Liu T.C.: 'Experimental evaluation of adsorption behaviour of intermediates in anodic oxygen evolution at oxidized nickel surfaces', *J. Chem. Soc. Faraday Trans.*, 1987, **83**, pp. 1063–1080

[45] Druska P., Strehblow H.H., Golledge S.: 'A surface analytical examination of passive layers on CuNi alloys: Part I. Alkaline solution', *Corros. Sci.*, 1996, **38**, (6), pp. 835–851

[46] Jiang Y.X., Wang Y., Xu J.M., ET AL.: 'Electrocatalytic oxidation of carbon monoxide and methanol at Pt nanoparticles confined in SBA-15: voltammetric and in situ infrared spectroscopic studies', *J. Solid State Electrochem.*, 2005, **9**, (5), pp. 363–370

[47] Laviron E.: 'General expression of the linear potential sweep voltammogram in the case of diffusionless electrochemical systems', *J. Electroanal. Chem.*, 1979, **101**, pp. 19–28